Photophysics of the Interaction between a Fluorescein Derivative and Ficoll

ARTICLE *in* THE JOURNAL OF PHYSICAL CHEMISTRY A · NOVEMBER 2011

Impact Factor: 2.69 · DOI: 10.1021/jp204666j · Source: PubMed

THE JOURNAL OF PHYSICAL CHEMISTRY A

ARTICLE

pubs.acs.org/JPCA

Photophysics of the Interaction between a Fluorescein Derivative and Ficoll

Jose M. Paredes, Luis Crovetto, Angel Orte, Sergio G. Lopez, Eva M. Talavera, and Jose M. Alvarez-Pez*

Department of Physical Chemistry, University of Granada, Cartuja Campus, 18071 Granada, Spain

Supporting Information

ABSTRACT: Ficoll has been widely used as a crowding agent to mimic intracellular media because it is believed to be noninteracting and is composed of mixed sizes such that smaller and larger diffusing solutes can be studied. Due to the interest that the fluorescent dye 9-[1-(2-methyl-4-methoxyphenyl)]-6-hydroxy-3*H*-xanthen-3-one (TG-II) as a fluorometric probe of phosphate ions in intracellular media could generate, we describe the spectral characteristics of the system TG-II-Ficoll in aqueous solution by means of absorption spectroscopy, steady-state fluorescence, time-resolved fluorescence, time-resolved emission spectroscopy, and fluorescence lifetime correlation spectroscopy. The spectral characteristics found are consistent with the formation of an adsorption complex on the surface of Ficoll, probably due to hydrogen bonding between TG-II and Ficoll. In addition, the diffusion coefficient calculated for the association was similar to the diffusion coefficient previously recovered for Ficoll in the same experimental conditions. Therefore, our overall data clearly demonstrate that Ficoll is not an inert crowding agent when in the presence of fluorescein derivative dyes.

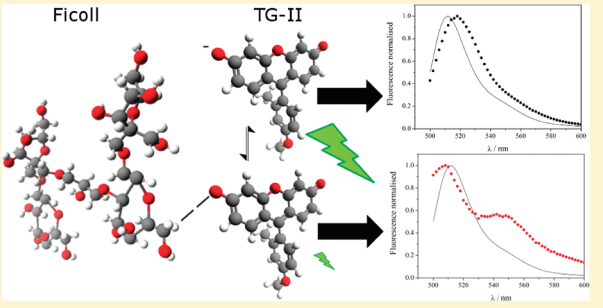

INTRODUCTION

The intracellular environment is highly crowded due to the presence of large amounts of soluble and insoluble biomolecules, including proteins, nucleic acids, ribosomes, and carbohydrates, meaning that a significant fraction of the intracellular space is not available to other macromolecular species. This implies a nonspecific influence of steric repulsions on specific reactions that occur in highly volume-occupied media; therefore, the structural properties observed in dilute buffer solutions in vitro do not represent the in vivo scenario.[1] Experimental and theoretical work has demonstrated the significant effects of macromolecular crowding on many biological processes in solution.[2] Some consequences of molecular crowding include altered chemical reaction rates and equilibrium constants,[3] enhanced protein folding,[4] and reduced solute diffusion.[5]

Macromolecular crowding in solution can be mimicked experimentally via the addition of high concentrations of inert synthetic or natural macromolecules, termed crowding agents, to systems in vitro. Ficoll has been widely used as a crowding agent because it is believed to be noninteracting and is composed of mixed sizes such that smaller and larger diffusing solutes can be studied.[5b,6] Other polymeric macromolecules, such as dextrans of different molecular weights, have also been used as crowding agents.[6]

To study molecular diffusion, protein dynamics, chemical reaction rates, or equilibrium constants in solutions that mimic cellular cytoplasm, fluorescence has been the most widely used spectroscopic method. Thus, fluorescence recovery after photobleaching (FRAP),[7] single-particle tracking (SPT),[8] fluorescence resonance energy transfer (FRET),[9] fluorescence correlation spectroscopy (FCS),[6] and fluorescence cross-correlation spectroscopy (FCCS)[10] have been extensively employed to investigate molecular mobility, transport and diffusion both in artificial systems and directly in living cells.

In a series of previously published papers, we showed by FCS and time-correlated single-photon counting (TCSPC) that the photophysical characteristics of 9-[1-(2-methyl-4-methoxyphenyl)]-6-hydroxy-3*H*-xanthen-3-one (TG-II), a dye corresponding to the so-called Tokyo Green family of fluorescein derivatives,[11] are highly sensitive to phosphate concentrations.[12] Specifically, the autocorrelation (AC) function and the fluorescence lifetime can be considered direct and sensitive means of investigating the environmental phosphate concentration in small volumes at near-physiological pH. Moreover, we have also employed fluorescence lifetime correlation spectroscopy (FLCS) to investigate specific ion effects on TG-II photophysics in aqueous solutions.[13] FLCS makes use of TCSPC information to extend the applicability of conventional FCS,[14] thus allowing for the determination of autocorrelation functions from different emitters by applying temporal filters based on the fluorescence decay.[15] The FLCS methodology has been shown to be a valuable tool for studies with TG-II because its fluorescence lifetime is 3.71 ns when the xanthene moiety is in the anion form and is reduced to 0.20 ns when the dye is protonated at acidic pH values.[12a]

Received: May 19, 2011
Revised: September 27, 2011
Published: October 05, 2011

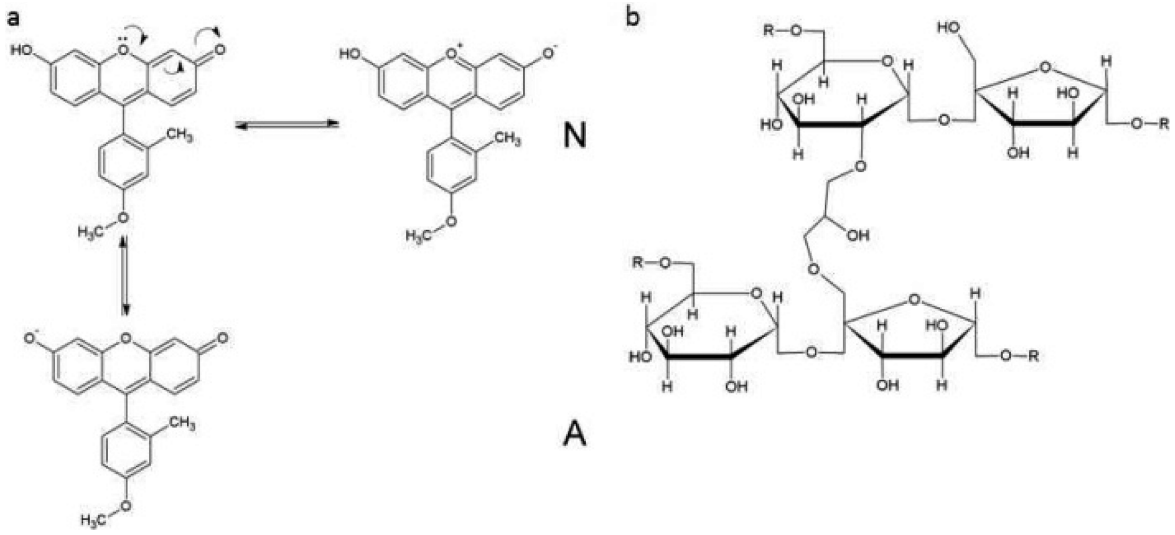

Figure 1. (a) Chemical structures and ground-state proton-exchange reaction of TG-II forms at near-neutral pH. N (neutral) and A (anion). (b) Chemical structural unit of a Ficoll macromolecule.

Due to the interest that the use of TG-II as a fluorometric probe of phosphate ions in intracellular media could generate, in this paper, we report the behavior of the dye in aqueous solutions with Ficoll added to mimic the crowded cell environment. Previous studies have obtained the diffusion properties of a series of fluorescent dyes by FCS in the presence of crowding agents.[6] Moreover, fluorescein isothiocyanate (FITC) and Ficoll have been used to obtain measurements of the fractional clearances in isolated perfused rat kidneys.[16]

However, in the present paper, we show that Ficoll is not an inert crowding agent when in the presence of xanthenic dyes such as TG-II. We report on the behavior of the TG-II−Ficoll system, describing the spectral characteristics of this system in aqueous solution by means of absorption spectroscopy, steady-state fluorescence, time-resolved fluorescence, species-associated spectra (SAS) and FLCS.

EXPERIMENTAL SECTION

Materials and Methods. The fluorescent dye 9-[1-(2-methyl-4-methoxyphenyl)]-6-hydroxy-3*H*-xanthen-3-one (TG-II, Figure 1) was prepared according to the literature.[12a] The chemicals used were NaOH (Aldrich, spectroscopic grade, platelets), $HClO_4$ (Aldrich, spectroscopic grade), and Ficoll 400 (Sigma, molecular biology grade, dialyzed and lyophilized). The Ficoll concentration is expressed as the Ficoll mass:water mass percentage. All chemicals were used as received without further purification.

Stock solutions of TG-II at different concentrations (2×10^{-4} M for ensemble-level measurements or 2×10^{-6} M for single-molecule experiments) and Ficoll (50% for the ensemble level or 20% for the single-molecule level) were prepared using Milli-Q water as the solvent. Appropriate concentrations of TG-II and Ficoll were prepared by mixing the required amounts of the stock solutions. To adjust the pH of the aqueous solutions, 0.01 M NaOH and 0.01 M $HClO_4$ in Milli-Q water were used. The solutions were kept cool in the dark when not in use to avoid possible deterioration through exposure to light and heat.

The refractive indices of the samples were recorded using an Abbe refractometer, model 51837 (Carl Zeiss) (Figure S-1, Supporting Information). Absorption spectra were recorded on a Perkin-Elmer Lambda 650 UV/vis spectrophotometer with a temperature-controlled cell. Steady-state fluorescence emission spectra were obtained using a JASCO FP-6500 spectrofluorometer equipped with a 450-W xenon lamp for excitation, with an ETC-273T temperature controller. Fluorescence decay traces at the ensemble level were recorded via the TCSPC method using a FluoTime 200 fluorometer (PicoQuant GmbH). The excitation source consisted of either a 440 nm or 470 nm LDH pulsed laser with a minimum pulse width of 68 or 73 ps, respectively. The pulse repetition rate was 20 MHz. Fluorescence decay histograms were collected at different emission wavelengths along 1320 channels (with a time increment of 36 ps per channel) using 10 × 10 mm cuvettes. Histograms of the instrument response functions (using LUDOX scatterer) and sample decays were recorded until they reached 2×10^4 counts in the peak channel. For SAS, the collection time for fluorescence decay recording was long enough to achieve more than 1×10^4 counts in the peak channel at $\lambda_{em} < 560$ nm and at least 2×10^3 counts in the 560−600 nm range.

Fluorescence fluctuation traces were recorded with a MicroTime200 fluorescence lifetime microscope system (PicoQuant GmbH) using the time-tagged time-resolved (TTTR) methodology, which permits the simultaneous recovery of fluorescence decay traces from molecules in the confocal volume.[17] The excitation source consisted of either the 440 or 470 nm LDH pulsed laser previously described. The light beam was directed onto a dichroic mirror (510dcxr) to the oil immersion objective (1.4 NA, 100×) of an IX-71 inverted microscope system (Olympus). The collected fluorescence light was filtered by an HP500LP long-pass filter (AHF/Chroma) and focused onto a confocal aperture. Beyond the aperture, the transmitted light was refocused onto two SPCM-AQR-14 single-photon avalanche diode (SPAD) detectors (Perkin-Elmer) after the signal was separated by a 50/50 beam splitter. Data acquisition was performed with a Timeharp 200 TCSPC module (PicoQuant GmbH) in TTTR mode, enabling a reconstruction of the lifetime histogram.

Data Analysis. The fluorescence decay traces at the ensemble level were individually analyzed in terms of exponential models using FluoFit software (PicoQuant GmbH). The tested decay

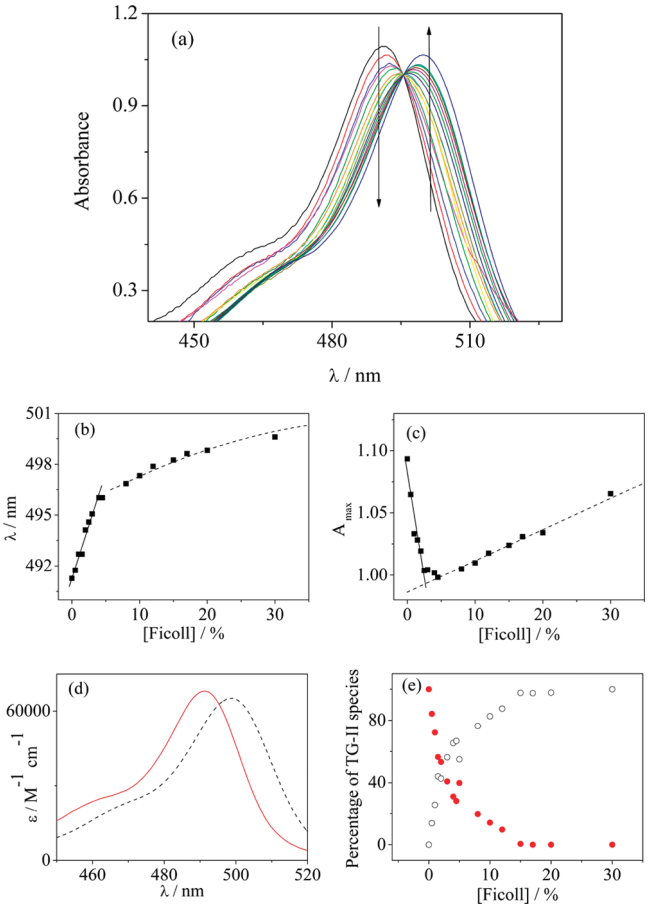

Figure 2. Absorption properties of TG-II (4×10^{-6} M) in crowded aqueous solution at pH = 9.5 in the presence of Ficoll concentrations between 0 and 30%. (a) Aborption spectra corresponding to 0, 0.5, 1, 1.5, 2, 3, 4, 4.5, 8, 10, 12, 15, 17, 20, and 30%. (b) Wavelength of the maximum absorbance, showing a bathochromic shift. (c) Absorbance of the peak maximum vs percentage of Ficoll based on the above spectra. (d) Molar absorption coefficients of TG-II free anion form (solid line) and TG-II—Ficoll interacting form (dashed line). (e) Percentages of TG-II as free anion form (filled circles) and interacting form (empty circles).

functions were monoexponential, biexponential, or triexponential. Fluorescence decay traces of solutions at the same pH and excitation wavelength were globally fitted with the decay times linked as shared parameters, whereas the pre-exponential factors were locally adjustable parameters. Any of the fitting parameters can be kept fixed during the fitting or can be freely adjustable to determine the optimum values.

The fluorescence decay traces at the single-molecule level were analyzed by means of the SymPhoTime software (PicoQuant GmbH) and by applying the maximum likelihood estimator (MLE), which yields the correct parameter set for low count rates.[18]

Fluorescence lifetime correlation spectroscopy (FLCS) is a method that uses time-correlated single-photon counting (TCSPC) information to extend the applicability of conventional fluorescence correlation spectroscopy, thus allowing for the determination of autocorrelation functions from different emitters by applying temporal filters based on the fluorescence decay. Assuming that the identified signal components are constant TCSPC patterns, FLCS makes it possible to simultaneously monitor the diffusion speed of two dyes with overlapping emission spectra and very similar diffusion coefficients. The analysis of FLCS curves was realized by using SymPhoTime software (PicoQuant GmbH). FLCS analysis starts with a preliminary inspection of the overall TCSPC histogram. In FLCS, each photon is assigned a probability of originating from a fluorescent species. From this probability, a filter function can be deduced. When the FLCS correlation curve is calculated, this filter function is used to weigh each individual photon on the basis of its TCSPC channel. Next, it is possible to calculate the diffusion coefficient of species i (D_i) using eq 1:

$$D_i = \frac{{\omega_0}^2}{4\tau_i} \quad (1)$$

where ω_0 is the effective lateral focal radius at an intensity of $1/e^2$; and τ_i is the diffusional time of species i. ω_0 and D_i are calculated on the basis of a reference dye, which, in our case, was the TG-II anion form.[12b] Due to the low fluorescence intensity of the dye—Ficoll interaction, FLCS curves were recorded three times with a measurement duration of 1 h each and then summed to obtain adequate bursts to build an acceptable AC function.

RESULTS AND DISCUSSION

Absorption Spectroscopy. The visible absorption spectra of aqueous solutions of TG-II and various Ficoll concentrations were recorded at pH 9.5 and 7.2. Figure 2a shows, as an example, the visible absorption spectra recorded for TG-II solutions (4×10^{-6} M) in the presence of different Ficoll concentrations in the range 0—30% at pH = 9.5. The addition of increasing amounts of Ficoll causes a continuous bathochromic shift of the band maximum (Figure 2b). With this addition, two trends can be observed; when the Ficoll concentration was increased to 4%, the absorbance at the maximum decreased, whereas from 4% and above, the addition of larger amounts of Ficoll caused a monotonous increase in the maximum absorbance (Figure 2c). The slope of the plot of the bathochromic shift vs Ficoll concentration shows a similar tendency, decreasing when the concentration is above 4% Ficoll (Figure 2b). The addition of Ficoll at pH 7.2 produced similar characteristics (Figure S-2, Supporting Information), but the increase in the shoulder absorbance at 465 nm with increasing Ficoll concentration is more pronounced. Furthermore, at the pH values studied, the addition of Ficoll at any fixed pH causes the appearance of an isosbestic point at 496 nm.

The experimental absorption spectra of aqueous solutions of TG-II in the 6.0—9.5 pH range show two spectroscopically distinguishable species: neutral (N) and anion (A) (Figure 1). At the basic pH level of 9.5, the aqueous absorption spectrum of free TG-II is essentially composed of a band characterized by a maximum at 490 nm and a small shoulder around 460 nm; at near-neutral pH values, the spectrum changes and the shoulder around 460 nm becomes more pronounced. For more acidic solutions, the absorption spectrum of the neutral form shows two absorption bands, with maxima at 453 and 477 nm.[12a] The TG-II spectra recorded at different Ficoll concentrations are consistent with the presence of two visible absorbent species in equilibrium, showing variable spectral characteristics with increasing Ficoll concentration. It is not likely that the TG-II neutral $\rightleftarrows$ anion reaction is implicated in these changes at pH 9.50 because the pK_a is 5.97[12a] and the neutral species should not be present. Therefore, the equilibrium established in the presence of Ficoll

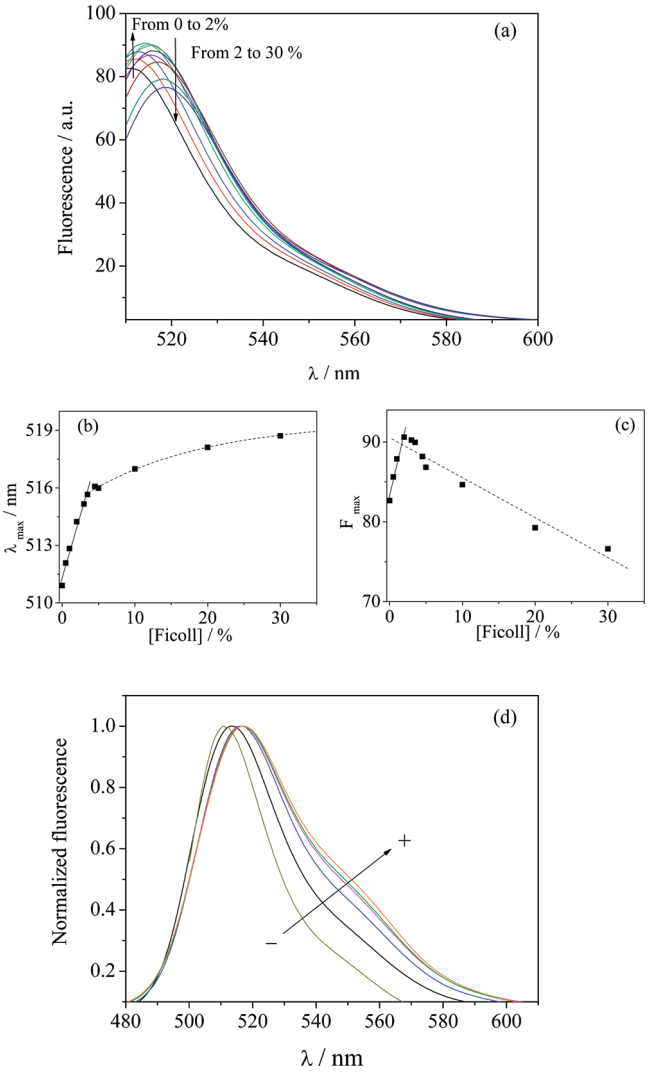

Figure 3. (a) Steady-state emission spectra (λ_{ex} = 496 nm) of 4×10^{-6} M TG-II aqueous solutions at pH = 9.5 and different Ficoll percentages in the 0−30% range. (b) Wavelength of the fluorescence maximum vs Ficoll percentage for the same spectra. (c) Intensity of fluorescence at the maximum vs Ficoll percentage for the same spectra. (d) Normalized fluorescence of TG-II at Ficoll concentrations of 0, 2, 10, 15, 20, and 30%. The arrow indicates the increment of Ficoll concentration.

between two different absorbers must involve the free anion form and a new association species produced by the dye−Ficoll interaction. To corroborate the number of absorbent species involved in this system and to quantify the assumed association between the dye and Ficoll, we have analyzed the absorption data by means of principal component analysis (PCA).[19−21] The use of two different absorbers explained 99.3% of the variation of the absorption spectra. The first absorber is predominant at very low or null Ficoll concentrations. Therefore, we assigned this spectral profile to the TG-II free anion form. On the contrary, the second species progressively appears with increasing Ficoll concentrations, so we assigned this absorber to the TG-II − Ficoll interacting form. Parts d and e of Figure 2 show the recovered molar absorption coefficients and percentages of TG-II as free anion form, and TG-II−Ficoll interacting form. It is evident from Figure 2e that at Ficoll concentrations above 17% nearly all TG-II molecules interact with the polymer.

Emission Spectroscopy. *Steady-State Fluorescence.* We collected steady-state emission spectra from TG-II aqueous solutions at pH = 9.5 in the presence of increasing concentrations of Ficoll in the range 0−30% using excitation at the isosbestic point (496 nm). The addition of Ficoll causes a progressive bathochromic shift of the fluorescence maximum (Figure 3a). Moreover, two regimes can be seen when the maximum emission wavelength is plotted versus the concentration of Ficoll, as a change in the slope of the plot is evident (Figure 3b), similar to that found in the absorption spectra. Figure 3b shows that, below 4% Ficoll, the bathochromic shift is very pronounced, but above 4% Ficoll, the slope decreases. In contrast, the intensity of the fluorescence signal showed the opposite behavior with respect to the absorbance. The addition of up to 2% Ficoll causes an increase in the fluorescence signal, whereas an increase in the Ficoll concentration to a range between 2 and 20% produces a slight decrease in the fluorescence signal (Figure 3c). At higher Ficoll concentrations (30%), a considerable quenching of the TG-II fluorescence emission can be observed along with an increase in the fluorescence emission at around 555 nm, as shown in Figure 3d where the spectra have been normalized to the emission maxima to better visualize the difference in the shoulders of the spectra. This shoulder at 555 nm is similar to the characteristic emission of TG-II at near-neutral and moderately acidic pH.

At neutral or moderately acidic pH, the addition of Ficoll to aqueous solutions of TG-II also causes a more evident increase in the fluorescence intensity of the shoulder around 555 nm. Furthermore, we observed the opposite behavior upon selecting different excitation wavelengths. At pH 5.5 and by preferentially exciting the anion form (490 nm), a fluorescence signal increase with the addition of Ficoll in the 0−2% range, along with a fluorescence decrease above 2%, similar to those at basic pH, can be observed (Figure S-3, Supporting Information). However, by preferentially exciting the neutral form (440 nm), only an increase in the intensity of the steady-state fluorescence signal at 515 nm and around the shoulder is observed (Figure S-4, Supporting Information).

Briefly, the steady-state fluorescence spectra recorded show that the addition of Ficoll to aqueous solutions of TG-II at either basic or near-neutral pH causes two different behaviors. At Ficoll concentrations above 2%, the maximum fluorescence signal decreases due to the formation of increased amounts of a species with spectral characteristics similar to those of the neutral TG-II, namely decreased fluorescence intensity at 490 nm and increased intensity at the shoulder (ca. 555 nm). In contrast, at concentrations below 2% Ficoll, an increase in the fluorescence signal at the maximum can be observed, possibly due to the protection from solvent quenching by Ficoll crowding, which masks the decreasing fluorescence signal due to the formation of the new less fluorescent species with spectral characteristics similar to those of the neutral TG-II.

Time-Resolved Fluorescence. More important experimental information on the interaction between TG-II and Ficoll is, however, accessible through time-resolved fluorescence measurements, through which insights into the behavior of the system in the excited state can be obtained. Fluorescence decay traces under different experimental conditions (i.e., the absence or presence of Ficoll at concentrations in the range between 0 and 30% and at different pH and λ_{em} values) were recorded to build a multidimensional decay trace surface, along with the

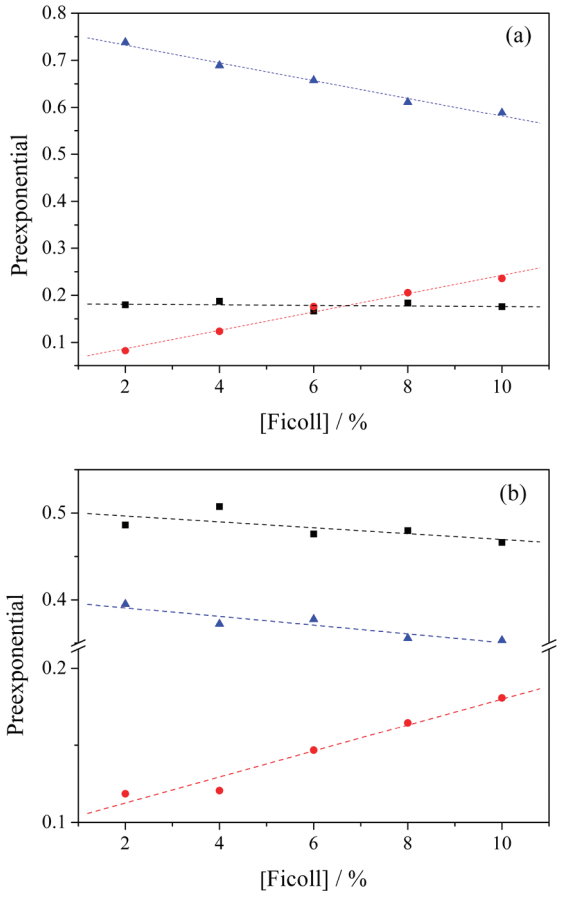

Figure 4. Normalized preexponentials recovered from the fitted fluorescence decay traces from 4×10^{-6} M TG-II crowded aqueous solutions at pH = 5.5 in the presence of increasing amounts of Ficoll. The experimental conditions were (a) λ_{ex} = 440 nm and λ_{em} = 550 nm and (b) λ_{ex} = 470 nm and λ_{em} = 550 nm. Key: ■ preexponential of the longest decay time, ▲ preexponential of the shortest decay time, and ● preexponential of the intermediate decay time.

fluorescence spectra obtained at discrete times during the fluorescence decay.

Decay traces from solutions at pH 9.50 and at the same Ficoll concentration but at different λ_{em} values were globally well fitted by biexponential functions, where the decay times, τ_i, were linked parameters and the preexponential factors were locally adjustable parameters. Biexponential functions turned out to be the best model to fit the experimental decay traces. A triexponential model did not improve the reduced χ_r^2 values. These results show that the two decay times were dependent on the Ficoll concentration when this is below 5%. However, above the 5% Ficoll concentration, the two decay times were effectively invariable with Ficoll content. Therefore, we performed a global analysis of all decay traces collected at Ficoll concentrations above 5% and the same pH, whereas for Ficoll concentrations below 5% the decay traces were independently fitted at each Ficoll concentration (Table S-1, Supporting Information). The results show a large decay time varying from 3.72 to 4.12 ns and a second decay time between 1.24 and 2.04 ns, depending on the Ficoll content. It should also be noted that a slight increase in the range of Ficoll concentration between 0 and 5% slightly increases the value of the longer decay time until it reaches the saturation value of 4.12 ns. The shorter decay time increases to 2.15 ns and then decreases to 1.91 ns with increasing Ficoll concentration up to 5%, after which it remains constant. It should be noted the preexponential factor of this last decay time is small. Therefore, it is more difficult to accurately estimate its value due to this low contribution.

When free in aqueous solution, TG-II shows mainly monoexponential behavior with a lifetime of 3.71 ± 0.30 ns, corresponding to the anionic species, at pH values above 6.20. Below pH 6.20, the decay behavior of the neutral form, with a decay time of 0.20 ± 0.01 ns, starts to become evident.[12a] In contrast, the addition of Ficoll causes the appearance of an intermediate decay time, whose value lies between those corresponding to the aqueous free TG-II anion and the neutral species. Therefore, we studied the fluorescence decay traces from solutions in the presence of Ficoll at pH values lower than 6.20. These decay traces were well fitted by using triexponential functions such that three different decay times were recovered (Table S-2, Supporting Information). Two of the decay times, 4.01 ± 0.02 and 1.60 ± 0.05 ns, were similar to those obtained under a basic pH, and the third decay time, 0.27 ± 0.02 ns, was in the same range as that of the free neutral species. We also observed the behavior of the normalized preexponentials corresponding to each decay time with the addition of Ficoll. Figure 4 shows the normalized values recovered from solutions at pH 5.50 with increasing Ficoll concentrations and excitation at 440 and 470 nm, which preferentially excites either the neutral or anion forms, respectively. In all cases, the preexponential factor of the shorter decay time tends to decrease with increasing Ficoll concentration, whereas that of the intermediate decay time increases with increasing Ficoll concentration. The preexponential factor corresponding to the longer decay time appears to decrease slightly (Supporting Information Figures S-5, S-6, and S-7 show the preexponentials at different excitation and emission conditions).

Time-Resolved Emission Spectroscopy. Because each species is characterized by one lifetime that is significantly different from that of the others, it is possible to decompose the overall emission spectrum into various components. To accomplish this, we performed the species-associated spectra (SAS) to gain more insight into the spectral characteristics of the species in the system.[22] Decay traces from aqueous solutions of TG-II at pH 5.8 in the presence of Ficoll were recorded at an excitation wavelength of 470 nm and an emission wavelength in the 500–600 nm range using 2 nm steps. The complete data matrix available can be described by a three-dimensional surface $I(\lambda_{em},t)$ representing the fluorescence intensity at all emission wavelengths and times during the fluorescence decay. It should be mentioned that, above 560 nm, the decay traces had very low fluorescent signals; however, the signals are not sufficiently strong to alter the shapes of the spectra recovered because they are the tails of broad spectral profiles. All of the traces were recorded for the same collection time, and hence, the product of the normalized preexponential coefficients at each wavelength and the lifetime is proportional to the steady-state fluorescence intensity of the species with that lifetime, as indicated by eq 2.

$$f_{i,\lambda} = \frac{\alpha_{i,\lambda}\tau_i}{\sum_i \alpha_{i,\lambda}\tau_i} \qquad (2)$$

where $f_{i,\lambda}$ is the fractional intensity of species i, $\alpha_{i,\lambda}$ is the preexponential factor of i at wavelength λ, and τ_i is the lifetime of species i.

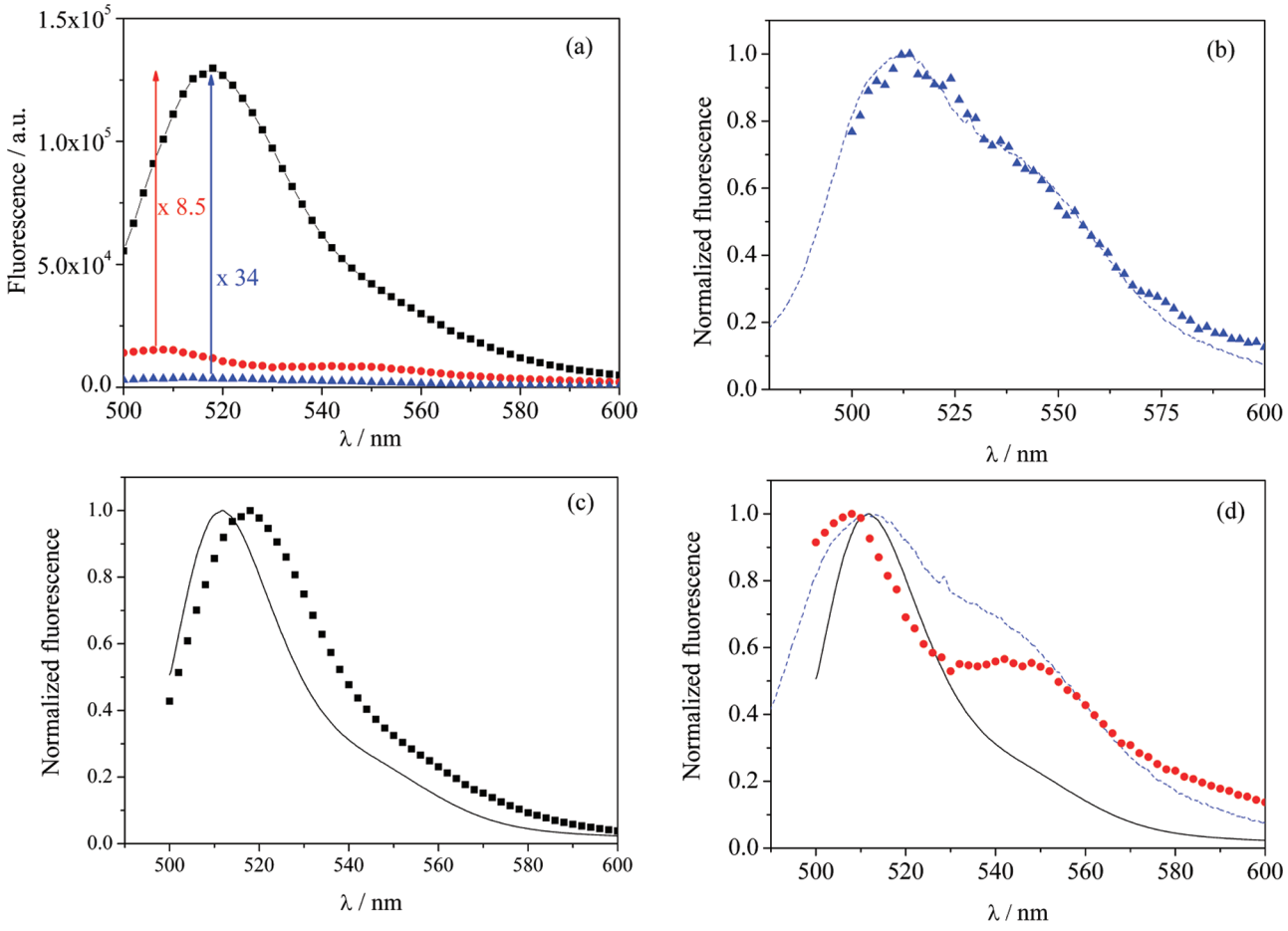

Figure 5. (a) SAS profiles of the different lifetime components: 0.2 (▲), 1.91 (●), and 4.12 (■) ns. The factors indicate the values necessary to normalize the spectra. (b) Normalized spectrum from the 0.20 ns lifetime component (▲) and emission spectrum of the free neutral TG-II in aqueous solution (dashed line). (c) Normalized spectrum from the 4.12 ns lifetime component (■) and emission spectrum recorded for the free aqueous TG-II anion (solid line). (d) Normalized spectrum from the 1.91 ns lifetime component (●) and emission spectra recorded for neutral (dashed line) and free aqueous anion TG-II (solid line).

Figure 5a shows the SAS generated for the three lifetime components (0.20, 1.91, and 4.12 ns). In Figure 5b, the recovered fluorescence spectra for the 0.20 ns lifetime component is compared with the spectral emission shape of the free neutral species in aqueous solution. It can be observed that the correspondence is very good. Figure 5c shows the recovered fluorescence spectra from the 4.12 ns component for the same experiment and the spectrum recorded from TG-II at a basic pH (free anion). There is a red shift in the SAS band with respect to the aqueous free anion, but the shapes are similar for both spectra. This is consistent with the red shift of the emission spectra with increasing Ficoll concentration (Figure 3a). Finally, Figure 5d shows the recovered fluorescence spectra for the 1.91 ns component. This profile clearly does not match the spectra from either the aqueous free neutral or anionic species. This suggests that the species associated with the 1.91 ns lifetime is a completely different form of TG-II. Similar fluorescence spectral shapes were obtained by carrying out SAS experiments at a basic pH, although in this case, only two decay times appeared. The two spectral profiles recovered were those corresponding to the anion form (red-shifted) and the 1.91 ns component due to the TG-II−Ficoll interaction species.

Fluorescence Lifetime Correlation Spectroscopy (FLCS). The key observable in FCS is the intensity fluctuation in the fluorescence signal. In the absence of photophysical processes affecting these intensity fluctuations along with the standard case of an assumed prolate ellipsoidal Gaussian observation volume, the autocorrelation (AC) function responds to the following equation:[23]

$$G_D(t) = \frac{1}{\langle N \rangle}\left(1 + \frac{t}{\tau_D}\right)^{-1}\left(1 + \frac{t}{\tau_D \omega^2}\right)^{-1/2} \quad (3)$$

in which t is the correlation lag time; $\omega = z_0/\omega_0$ is the ratio between the effective focal radius along the optical axis, z_0, and the lateral focal radius, ω_0, both at an intensity of $1/e^2$; τ_D represents the diffusion time; and $\langle N \rangle$ is the average number of molecules in the probe volume, which can be calculated from the initial correlation amplitude $G_D(t=0)$.

If, in addition to diffusional motion, the fluctuations are also caused by transitions between bright and dark states due to some photophysical process of the fluorophore, the AC function can be

dx.doi.org/10.1021/jp204666j |J. Phys. Chem. A 2011, 115, 13242–13250

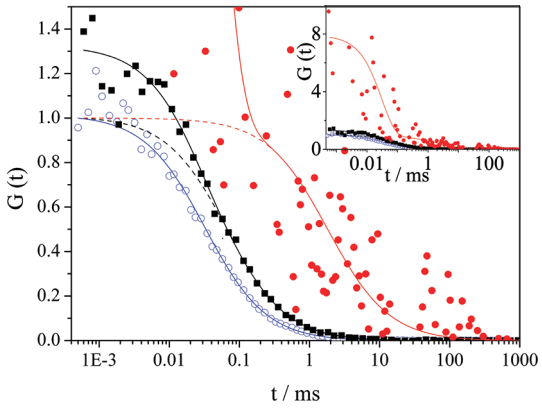

Figure 6. FLCS function of 2 nM TG-II at basic pH in aqueous solution without Ficoll (D = 330 $\mu m^2/s$) (○). 10 nM TG-II at pH = 9.70 in 2% Ficoll, selecting the 4.12 ns lifetime component (D = 174 $\mu m^2/s$) (■) and selecting the 1.91 ns lifetime component (D = 20.1 $\mu m^2/s$) (●). λ_{ex} = 470 nm. The dashed line represents the diffusion process.

described by[23]

$$G(t) = G_D(t)\frac{1}{1-f}(1-f+fe^{-t/\tau_i}) \quad (4)$$

in which the transition time to the dark state, τ_i, represents the interconversion time between the bright and dark species, and f is the fraction of molecules in the dark state.

The FLCS methodology can be used to filter the different contributions from species with different lifetimes, allowing for the calculation of a separate AC function for each signal component.[14,15] From the TCSPC information, temporal weighting filters were estimated for each component, in our case, background photons and photons arising from the TG-II neutral form, the anionic form, and the new species arising from the interaction between Ficoll and the dye. We used an excitation laser power of <5.6 μW to avoid both photobleaching and triplet population.[12b] The AC curve of the TG-II anion in aqueous solution at pH 9.5 obtained by FLCS for the 3.8 ns component shows pure diffusional behavior that could be well fitted with eq 3 (Figure 6), therefore confirming the absence of a proton-transfer reaction. The diffusional term was characterized by a time, τ_D, of 0.023 ms, which corresponds to a diffusion coefficient of 330 $\mu m^2/s$.[12b] To study the effect of the addition of Ficoll to aqueous solutions of TG-II, we recorded fluorescence fluctuation traces from 1.0 × 10^{-8} M TG-II nonbuffered solutions at pH values of 9.70 and 6.10. Figure 6 shows the TG-II lifetime-filtered AC function for the 4.12 and 1.91 ns lifetime components for TG-II solutions with 2% Ficoll at pH 9.70, along with the AC function for the free TG-II anion in the absence of Ficoll. As shown in Figure 6, the addition of Ficoll results in a dramatic change in the TG-II anion AC function. Two transitions occur in the AC function of the TG-II species in the presence of Ficoll. There is an exponential decay in the microsecond time range and in the diffusional part, which lies in the millisecond range (Figure 6). Similar results were found at pH 6.10 (Figure S-8, Supporting Information). By fitting the AC curves to eq 4, we recovered the transition time to a dark state, τ_i, and the diffusion time, τ_D. The value of τ_i represents the interconversion kinetics from one species to each other because, once the contribution of a species is filtered out, it acts as a dark state for the form remaining in the FLCS AC curve. We recovered the values for the transition rate constants, k_i, defined as $1/\tau_i$, for both the 4.12 and 1.91 ns lifetime components. For instance, at pH 9.70 and 2% Ficoll, the k_i value for the 4.12 ns lifetime component was 4.3 × 10^4 s^{-1}, with a dark fraction of 0.23, whereas it was 5.3 × 10^4 s^{-1} with a dark fraction of 0.84 for the 1.91 ns component. Both rates are in good agreement, suggesting that the interconversion process between the 4.12 ns component and the 1.91 ns component is the same. These interconversion rates are of the same order of magnitude as the protonation/deprotonation rate found between the TG-II anion/neutral in solution at pH 6.10, which was 6.3 × 10^4 s^{-1}.[13]

We then analyzed the diffusional behavior of the TG-II species in the presence of Ficoll. At pH 9.70, the diffusion coefficient for the 4.12 ns lifetime component in the presence of 2% Ficoll decreased to 173 ± 2.2 $\mu m^2/s$. This is in agreement with the finding of Dauty and Verkman, who reported that the diffusion coefficients of small molecules in Ficoll-70 solution were reduced in an exponential manner with respect to that in water.[6] Moreover, we also found a slow diffusion time for the 1.91 ns component lifetime, a component that we assign to the complex formed between Ficoll and the dye. This diffusion time was 1.83 ± 0.72 ms, a value over 40 times slower than that of the free anion in the presence of Ficoll and almost 2 orders of magnitude slower than that of the free anion in aqueous solution. The corresponding diffusion coefficient of this species was 20.1 ± 5.0 $\mu m^2/s$ at high pH and 21.3 ± 3.4 $\mu m^2/s$ at pH 6.10. Lavrenco et al. found a diffusion coefficient of 23 $\mu m^2/s$ from unfractionated samples of Ficoll 400 in water.[24] This similar diffusion coefficient value for the 1.91 ns component in comparison to the diffusion coefficient of Ficoll is consistent with the formation of an adsorption complex on the surface of Ficoll, probably due to hydrogen bonding between the hydroxyl group of TG-II and the numerous oxygen atoms of the hydroxyl residues of the polymer. According to this proposed structure, the spectral properties of TG-II in the complex would be intermediate between those of the neutral and anion forms of TG-II. In fact, the shape of this steady-state fluorescence spectrum (Figure 5) is similar to that of TG-II when the oxygen of the hydroxyl group is either linked to another chemical group or simply protonated at acidic pH values.[11,12] Nevertheless, the lifetime of the adsorption complex is larger than that of the neutral species, indicating that the bonding to the Ficoll surface is not covalent.

System Fluorescein—Ficoll. Absorption and Steady-State Emission Spectroscopy. We hypothesized that the interaction between TG-II and Ficoll is due to hydrogen bonding; therefore, it should be a general effect in other parent compounds. To test this assertion, we investigated whether the interaction of TG-II and Ficoll takes place with other xanthene derivatives, specifically the broadly used fluorescein dye. We recorded both the absorption and steady-state emission spectra from aqueous solutions of fluorescein in the presence of Ficoll at the same concentration range used in the previous experiments (0−30%), and pH 9.5. The spectra are shown in Figures S-9 and S-10 of the Supporting Information. As the concentration of Ficoll increases, both sets of spectra show features and trends similar to those observed with TG-II. Nevertheless, the existence of two anionic species in equilibrium derived from the ionization of fluorescein in aqueous solution, along with the close value of the lifetimes of these anionic species,[25] makes it practically unfeasible to conduct a similar study as was carried out with the fluorescein derived TG-II. Even though, from the results obtained, we can state that fluorescein interacts with Ficoll originating both absorption and

emission spectra altered in a similar way as happens with TG-II. So, one could assume that the interaction of Ficoll and xanthenes derivatives is widespread.

CONCLUSIONS

The isosbestic point visualized in the absorption spectra, the different steady-state fluorescence spectra observed when the Ficoll concentration is sufficiently high, and the consistent lifetime of 1.91 ns recovered from solutions in the presence of Ficoll indicate the formation of a new species between TG-II and Ficoll in aqueous solution. Moreover, the use of SAS permitted a determination of the steady-state emission spectrum corresponding to the 1.91 ns component and, therefore, that of the new species. The comparison of this spectrum with those of the other prototropic forms from TG-II makes evident the similarity with the spectrum from TG-II when its oxygen is either linked to another chemical group or simply protonated at acidic pH values. Finally, by using FLCS, we obtained lifetime-filtered AC functions for the 4.12 and 1.91 ns lifetime components from TG-II solutions in the presence of Ficoll. We calculated their diffusion coefficients and compared them with that from the free anion in the absence of Ficoll. The addition of Ficoll resulted in a dramatic decrease in the diffusion coefficient of the TG-II anion. Importantly, the diffusion coefficient of the 1.91 ns lifetime component was similar to the diffusion coefficient previously recovered for Ficoll. These findings are consistent with the formation of an adsorption complex on the surface of Ficoll, probably due to hydrogen bonding between TG-II and Ficoll. In addition, the system Ficoll−fluorescein shows spectral behavior similar to that observed with TG-II, suggesting that the interaction between Ficoll and xanthenes derivatives is widespread. Therefore, our overall data clearly demonstrate that extreme caution must be exercised in the interpretation of fluorescence data from xanthenic dyes in macromolecular crowding experiments, because Ficoll is not an inert agent when in the presence of such dyes.

ASSOCIATED CONTENT

Supporting Information. Study of refractive indices at different Ficoll concentrations. Figure S2 shows absorption spectra at different Ficoll concentrations. Figures S3 and S4 show fluorescence spectra at different λ_{ex} and different Ficoll concentrations. Figures S5, S6, and S7 show the preexponential at different λ_{ex} and λ_{em}. Figure S8 shows FLCS function at pH = 6.10. Figures S9 and S10 show absorption and steady-state emission spectra of fluorescein added to Ficoll. Tables S1 and S2 show decay times recovered by fitting of decay traces from solutions of TG-II with added Ficoll. This material is available free of charge via the Internet at http://pubs.acs.org.

AUTHOR INFORMATION

Corresponding Author

*E-mail: jalvarez@ugr.es. Fax: +34-958-244090. Tel: +34-958-243831.

ACKNOWLEDGMENT

This work was supported by grants CTQ2010-20507/BQU from the Ministerio Español de Ciencia e Innovación (cofinanced by FEDER funds) and P07-FQM-3091 from the Consejería de Innovación, Ciencia y Empresa (Junta de Andalucía).

REFERENCES

(1) Minton, A. P.; Wilf, J. Effect of macromolecular crowding upon the structure and function of an enzyme: Glyceraldehyde-3-phosphate dehydrogenase. *Biochemistry* **1981**, *20*, 4821–4826.

(2) Cheung, M. S.; Klimov, D.; Thirumalai, D. Molecular crowding enhances native state stability and refolding rates of globular proteins. *Proc. Natl. Acad. Sci. U. S. A.* **2005**, *102*, 4753–4758.

(3) Minton, A. P. The influence of macromolecular crowding and macromolecular confinement on biochemical reactions in physiological media. *J. Biol. Chem.* **2001**, *276*, 10577–10580.

(4) Martin, J.; Hartl, F. U. The effect of macromolecular crowding on chaperonin-mediated protein folding. *Proc. Natl. Acad. Sci. U. S. A.* **1997**, *94*, 1107–1112.

(5) (a) Seksek, O.; Biwersi, J.; Verkman, A. S. Translational diffusion of macromolecule-sized solutes in cytoplasm and nucleus. *J. Cell Biol.* **1997**, *138*, 131–142. (b) Dix, J. A.; Verkman, A. S. Crowding effects on diffusion in solutions and cells. *Annu. Rev. Biophys.* **2008**, *37*, 247–263.

(6) Dauty, E.; Verkman, A. S. Molecular crowding reduces to a similar extent the diffusion of small solutes and macromolecules: measurement by fluorescence correlation spectroscopy. *J. Mol. Recognit.* **2004**, *17*, 441–447.

(7) Verkman, A. S. Diffusion in cells measured by fluorescence recovery after photobleaching. *Methods Enzymol.* **2003**, *360*, 635–648.

(8) Jin, S.; Verkman, A. S. Single particle tracking of complex diffusion in membranes: simulation and detection of barrier, raft, and interaction phenomena. *J. Phys. Chem. B* **2007**, *111*, 3625–3632.

(9) Jares-Erijman, E. A.; Jovin, T. M. FRET imaging. *Nat. Biotechnol.* **2003**, *21*, 1387–1395.

(10) Bacia, K.; Kim, S. A.; Schwille, P. Fluorescence cross-correlation spectroscopy in living cells. *Nat. Methods* **2006**, *3*, 83–89.

(11) Urano, Y.; Kamiya, M.; Kanda, K.; Ueno, T.; Hirose, K.; Nagano, T. Evolution of Fluorescein as a Platform for Finely Tunable Fluorescence Probes. *J. Am. Chem. Soc.* **2005**, *127* (13), 4888–4894.

(12) (a) Paredes, J. M.; Crovetto, L.; Rios, R.; Orte, A.; Alvarez-Pez, J. M.; Talavera, E. M. Tuned lifetime, at the ensemble and single molecule level, of a xanthenic fluorescent dye by means of a buffer-mediated excited-state proton exchange reaction. *Phys. Chem. Chem. Phys.* **2009**, *11* (26), 5400–5407. (b) Paredes, J. M.; Orte, A.; Crovetto, L.; Alvarez-Pez, J. M.; Rios, R.; Ruedas-Rama, M. J.; Talavera, E. M. Similarity between the kinetic parameters of the buffer-mediated proton exchange reaction of a xanthenic derivative in its ground- and excited-state. *Phys. Chem. Chem. Phys.* **2010**, *12*, 323–327.

(13) Paredes, J. M.; Crovetto, L.; Orte, A.; Alvarez-Pez, J. M.; Talavera, E. M. Influence of the solvent on the ground- and excited-state buffer-mediated proton-transfer reactions of a xanthenic dye. *Phys. Chem. Chem. Phys.* **2011**, *13* (4), 1685–1694.

(14) Böhmer, M.; Wahl, M.; Rahn, H. J.; Erdmann, R.; Enderlein, J. Time-resolved fluorescence correlation spectroscopy. *Chem. Phys. Lett.* **2002**, *353*, 439–445.

(15) (a) Benda, A.; Fagul'ová, V.; Deyneka, A.; Enderlein, J.; Hof, M. Fluorescence Lifetime Correlation Spectroscopy Combined with Lifetime Tuning: New Perspectives in Supported Phospholipid Bilayer Research. *Langmuir* **2006**, *22* (23), 9580–9585. (b) Kapusta, P.; Wahl, M.; Benda, A.; Hof, M.; Enderlein, J. Fluorescence Lifetime Correlation Spectroscopy. *J. Fluoresc.* **2007**, *17*, 43–48. (c) Gregor, I.; Enderlein, J. Time-resolved methods in biophysiscs.3. Fluorescence lifetime correlation spectroscopy. *Photochem. Photobiol. Sci.* **2007**, *6*, 13–18. (d) Ray, K.; Zhang, J.; Lakowicz, J. R. Fluorescence Lifetime Correlation Spectroscopic Study of Fluorophore-Labeled Silver Nanoparticles. *Anal. Chem.* **2008**, *80* (19), 7313–7318. (e) Chen, J.; Irudayaraj, J. Fluorescence Lifetime Cross Correlation Spectroscopy Resolves EGFR and Antagonist Interaction in Live Cells. *Anal. Chem.* **2010**, *82* (15), 6415–6421. (f) Rüttinger, S.; Kapusta, P.; Patting, M.; Wahl, M.; Macdonald, R. On the Resolution Capabilities and Limits of Fluorescence Lifetime Correlation Spectroscopy (FLCS) Measurements. *J. Fluoresc.* **2010**, *20* (1), 105–114.

(16) Ohlson, M.; Sörensson, J.; Haraldsson, B. Glomerular size and charge selectivity in the rat as revealed by FITC-Ficoll and albumin. *Am. J. Physiol. Renal Physiol.* **2000**, *279*, F84–F91.

(17) Wahl, M.; Erdmann, R.; Lauritsen, K.; Rahn, H. J. Hardware solution for continuous time-resolved burst detection of single molecules in flow. *Proc. SPIE* **1998**, *3259*, 173–178.

(18) (a) Maus, M.; Cotlet, M.; Hofkens, J.; Gensch, T.; De Schryver, F. C.; Schafer, J.; Seidel, C. A. M. An experimental comparison of the maximum likehood estimation and nonlinear least-squares fluorescence lifetime analysis of single molecules. *Anal. Chem.* **2001**, *73*, 2078–2086. (b) Edel, J. B.; Eid, J. S.; Meller, A. Accurate Single Molecule FRET Efficiency Determination for Surface Immobilized DNA Using Maximum Likelihood Calculated Lifetimes. *J. Phys. Chem. B* **2007**, *111* (11), 2986–2990.

(19) Mandal, A. K.; Pal, M. K. Principal component analysis of the absorption spectra of the dye thiacyanine in the presence of the surfactant AOT: Precise Identification of the Dye-Surfactant Aggregates. *J. Colloid Interface Sci.* **1997**, *192*, 83–93.

(20) Al-Soufi, W.; Novo, M.; Mosquera, M. Principal component global analysis of fluorescence and absorption spectra of 2-(2′-Hydroxyphenyl)benzimidazole. *Appl. Spectrosc.* **2001**, *55*, 630–636.

(21) Ruedas-Rama, M. J.; Alvarez-Pez, J. M.; Orte, A. Formation of stable BOBO-3 H-aggregate complexes hinders DNA hybridization. *J. Phys. Chem. B* **2010**, *114*, 9063–9071.

(22) Valeur, B. *Principles of steady-state and time-resolved fluorometric techniques in Molecular fluorescence: Principles and applications*. Wiley-VCH Verlag Gmbh: Weingheim (Germany), 2001, pp 155−199.

(23) Haustein, E.; Schwille, P. Fluorescence Correlation Spectroscopy: Novel Variations of an Established Technique. *Annu. Rev. Biophys. Biomol. Struct.* **2007**, *36*, 151–169.

(24) Lavrenko, P. N.; Mikriukova, O. I.; Okatova, O. V. On the separation ability of various Ficoll gradient solutions in zonal centrifugation. *Anal. Biochem.* **1987**, *166*, 287–297.

(25) Alvarez-Pez, J. M.; Ballesteros, L.; Talavera, E. M.; Yguerabide, J. Fluorescein Excited State Proton Exchange Reactions: Nanosecond Emission Kinetics and Correlation with Steady State Fluorescence Intensity. *J. Phys. Chem. A* **2001**, *105*, 6320–6332.